CLM - R 168

CLM - R 168

UKAEA

Report

AN ELECTRO-OPTICAL SHUTTER FOR PRODUCING VARIABLE DURATION CO_2 LASER PULSES WITH SUB-NANOSECOND RISE TIME

T STAMATAKIS
A C SELDEN

CULHAM LABORATORY
Abingdon Oxfordshire

1977

Available from H. M. Stationery Office

C/18

£1.00

CLM-R168

AN ELECTRO-OPTICAL SHUTTER FOR PRODUCING VARIABLE DURATION CO_2 LASER PULSES WITH SUB-NANOSECOND RISETIME

by

T. STAMATAKIS *
A. C. SELDEN

ABSTRACT

An electro-optical shutter is described which, in conjunction with a CO_2 laser, generates laser pulses of variable duration and sub-nanosecond rise time. The design and operation of the shutter are presented in detail, starting from first principles. The effects of crystal quality — in terms of residual birefringence — and variation of spark-gap parameters — voltage, gap length, gas pressure — on its performance are fully investigated and the choice of gas filling and electrode material discussed. The device has been used to generate ~ 1 ns pulses in a CO_2 laser system.

* On attachment from Royal Holloway College,
University of London, Egham, Surrey, U.K.

UKAEA Culham Laboratory,
Abingdon,
Oxon OX14 3DB,
United Kingdom

April, 1977

SBN 85311 051 4

Corrigenda (October 1977)

Page 14	line 37	-	(Section 7) should read (Section 12)
Page 16	line 29	-	ref. (10) should be (6)
Page 19	line 14	-	refs. (10, 20, 23) should be (6, 20, 24)
Page 20	line 10	-	$\sim 10^8$ should read $\sim 10^7$

CONTENTS

1. INTRODUCTION

The generation of laser pulses with sub-nanosecond rise-time and variable duration requires the use of an optical modulator which is based on a physical effect fast enough to respond to GHz frequencies. Modulation at these frequencies can be achieved by utilizing the electro-optical effect. For example, if an electro-optical crystal is placed between crossed polarizers, the time variation of the applied electric field will be imposed upon any light passing through the system. Thus, in particular, the duration of a transmitted laser pulse can be reduced by suitable control of the potential difference across the crystal, usually in the form of a high voltage pulse derived from a transmission line. The obvious requirements of (a) a high degree of synchronization between the laser and electrical pulse, and (b) sub-nanosecond rise-time and jitter, can be satisfied by using a laser-triggered spark-gap (LTSG). In this device, the laser beam itself triggers a d.c.-charged high-pressure spark-gap. The combination of electro-optical crystal between crossed polarizers and the LTSG comprises an electro-optical shutter.

It is the purpose of this report to analyse all the design considerations for an electro-optical shutter and to present the subsequent results. These results particularly concern: (a) the performance of an electro-optical shutter using single crystals of high-resistivity GaAs, suitable for CO_2 laser radiation of 10μm wavelength; (b) the experimental assessment of three GaAs crystals, based upon their ability to discriminate against unwanted radiation (extinction ratio); and (c) the operational characteristics of a pressurised LTSG.

Although this shutter was specially constructed to suit 10μm radiation, the same design considerations can apply to any electro-optical shutter using crystals which belong (as does GaAs) to the $\bar{4}3m$ crystallographic point group of the cubic system.

2. LIGHT PROPAGATION IN CRYSTALS

An electro-optical shutter requires the optical components to be arranged in such a way that no light can be transmitted through the shutter unless an electric field is present. One such arrangement could be to place an electro-optical isotropic crystal between two polarizers whose transmission axes form a 90° angle, (Fig.1). This crystal, under the influence of an electric field, becomes anisotropic and the transmission of the system is no longer zero but controlled by the applied electric field.

In order to describe the operation of the electro-optical shutter, it is therefore necessary to summarize the main features of light propagation in both isotropic and anisotropic media.

2.1 Isotropic Media

The optical isotropy of a medium is the result of its dielectric properties which could be described in a linear relation between an electric field $\overline{E}$ (e.g. the $\overline{E}$ field of the electro-magnetic radiation incident on the crystal) and the resultant electric displacement $\overline{D}$.

$$\overline{D} = \varepsilon \varepsilon_o \overline{E} \ . \qquad (1)$$

The scalar quantity ε is the dielectric constant, or the relative permittivity of the medium, while ε_o is the permittivity of the free space. Using Maxwell's equations, it

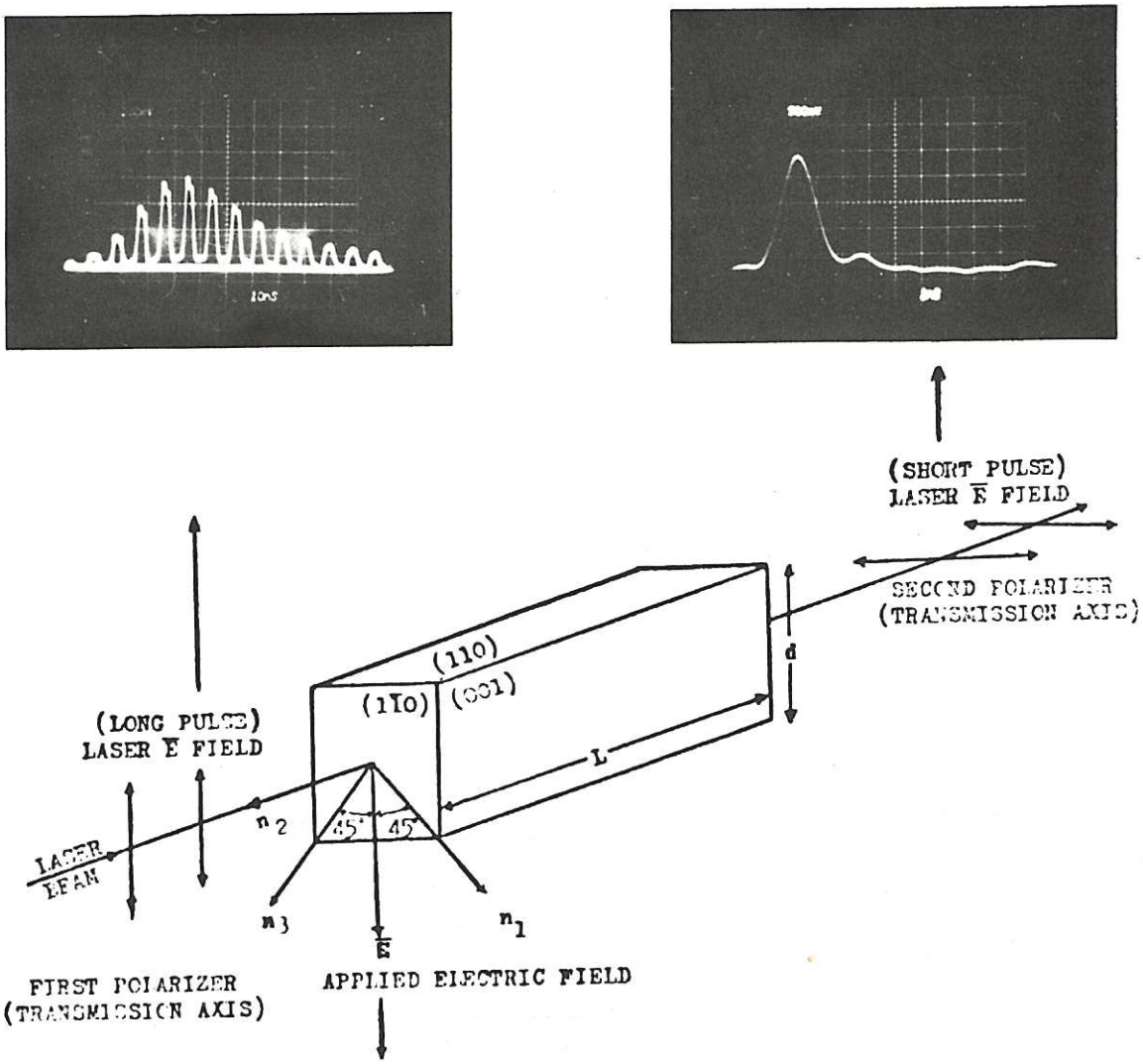

Fig.1

Optimum orientation of the GaAs crystal relative to: the polarization of the incident laser pulse (top left 10 ns/div); and the direction of the applied voltage pulse (bottom 2 ns/div). Top right oscillogram shows the generated ns laser pulse (1 ns/div).

could be shown that electro-magnetic radiation of any state of polarization is propagated unchanged through media for which equation (1) applies with phase velocity $U = c/\sqrt{\epsilon} = c/\eta$, irrespective of the direction of propagation.

2.2 Anisotropic Media

Equation (1) cannot describe the dielectric properties of either an isotropic electro-optic material, when an electric field is present, or any natural anisotropic medium. To describe the dielectric properties in either case, one needs to employ a new relation between $\overline{D}$ and $\overline{E}$ in which each component of $\overline{D} = [D_1, D_2, D_3]$ is linearly related to all three components of $\overline{E} = [E_1, E_2, E_3]$

$$\begin{aligned} D_1 &= \epsilon_0(\epsilon_{11}E_1 + \epsilon_{12}E_2 + \epsilon_{13}E_3) \\ D_2 &= \epsilon_0(\epsilon_{21}E_1 + \epsilon_{22}E_2 + \epsilon_{23}E_3) \\ D_3 &= \epsilon_0(\epsilon_{31}E_1 + \epsilon_{32}E_2 + \epsilon_{33}E_3) \end{aligned} \qquad (2)$$

The nine quantities ϵ_{ij} are constants of the medium. In order to specify the dielectric properties of an anisotropic medium, one has to specify the nine coefficients $\epsilon_{11}, \epsilon_{12}, \ldots$ which can be conveniently written in the form:

$$[\epsilon_{ij}] = \begin{bmatrix} \epsilon_{11} & \epsilon_{12} & \epsilon_{13} \\ \epsilon_{21} & \epsilon_{22} & \epsilon_{23} \\ \epsilon_{31} & \epsilon_{32} & \epsilon_{33} \end{bmatrix} .$$

The quantity $[\epsilon_{ij}]$ is called the dielectric tensor of the medium.

When equations (2) instead of (1) are used in conjunction with Maxwell's equations, it can be shown (Reference 1, p.671) that the structure of the anisotropic medium permits two linearly polarized plane electro-magnetic waves, with their directions of vibration mutually perpendicular, to travel with two different phase velocities in any given direction of propagation. The directions of the two permitted linear polarizations are determined by (a) the structure of the medium, (b) the direction of propagation, and (c) the direction of the external electric field. Plane electro-magnetic waves, linearly polarized along either of these directions, will emerge from the medium unchanged — just as if they had traversed an isotropic medium — and, for this reason, they are often called the privileged directions. If x and y denote the privileged directions for propagation along an axis z, then, x, y, z form a Cartesian system of coordinates.

Plane electro-magnetic waves linearly polarized along an arbitrary direction in the x,y plane, will, in general, emerge from the medium elliptically polarized. This could be visualized if one imagined the electro-magnetic wave resolved into two linearly-polarized components with their directions of vibration along x and y. The two components which travel with velocities U_1 and U_2, being in phase initially, will develop a continuously growing phase difference as they traverse the medium. These components emerging from the anisotropic medium, will retain their phase difference as they propagate in the surrounding isotropic medium and, therefore, the electro-magnetic wave that results from the recombining of the two out-of-phase components is elliptically polarized.

3. LIGHT TRANSMISSION THROUGH AN ELECTRO-OPTICAL SHUTTER

The operation of the electro-optical shutter is based upon the fact that when the anisotropy of the medium is electrically induced, the conversion of linearly into elliptically polarized light can be controlled electrically.

The transmission of radiation then is given by (see, for example, Ref. 1, p.696)

$$T = T_o \sin^2 2\varphi \sin^2 \frac{\delta}{2} \tag{3}$$

where φ is the angle between the transmission axis of the first polarizer and one of the privileged directions, and δ is the phase difference that has been developed between the two linearly polarized waves emerging from the electro-optical crystal. The factor T_o includes the effects of any reflection, diffraction or absorption loss in the crystal and the polarizers ($T_o = 1 - \alpha$ if α is the total loss). From equation (3) it can be seen that, for a given δ, the maximum transmittance of the electro-optical shutter occurs when $\varphi = 45^\circ$. The value of T increases as $\sin^2 \frac{\delta}{2}$ reaching its maximum value $T = T_o$ when $\delta = 180^\circ$.

The performance of an electro-optical switch is often limited because the value of the electric field required for inducing $\delta = 180^\circ$ is higher than that which could be applied to the crystal without the risk of dielectric breakdown. The value of δ, per unit length of the crystal, depends on the amplitude and direction of the electric field as well as on the direction of propagation. It will be shown later, that δ takes a maximum value (for a given field strength) when the field is applied along one particular $(h_1 k_1 \ell_1)$ axis of the crystal and, at the same time, light is propagated along another specific $(h_2 k_2 \ell_2)$ axis. It is therefore essential to find which two crystallographic axes fulfil this criterion so that an appropriately grown, cut and polished crystal can be used. It is also important to find the corresponding privileged directions so that the crystal can be so located between the two crossed polarizers that $\varphi = 45^\circ$.

4. INDEX ELLIPSOID

The propagation of light through an anisotropic medium may be illustrated and more easily understood if one employs a geometrical construction called the ellipsoid. This can be used to describe any crystal property given by a symmetrical second-rank tensor such as the dielectric tensor $[\varepsilon_{ij}]$. The symmetry of $[\varepsilon_{ij}]$, which is a consequence of Maxwell's equations (Ref.1, p.666), reduces the number of components of the tensor from nine to six (since $\varepsilon_{ij} = \varepsilon_{ji}$).

The most general form of the equation of the ellipsoid in Cartesian coordinates is:

$$\sum_{i,j=1}^{3} \frac{x_i x_j}{\varepsilon_{ij}} \equiv \frac{x_1^2}{\varepsilon_1} + \frac{x_2^2}{\varepsilon_2} + \frac{x_3^2}{\varepsilon_3} + 2\frac{x_1 x_2}{\varepsilon_{12}} + 2\frac{x_1 x_3}{\varepsilon_{13}} + 2\frac{x_2 x_3}{\varepsilon_{23}} = 1 . \tag{4}$$

However, there is always a system of Cartesian coordinates — the so-called system of principal dielectric axes — in which the above equation takes its simplest form:

$$\frac{x_1^2}{\varepsilon_1} + \frac{x_2^2}{\varepsilon_2} + \frac{x_3^2}{\varepsilon_3} = 1 . \tag{5}$$

The quantities $\varepsilon_i (i = 1,2,3)$ are then called the principal dielectric constants.

Replacing the dielectric constants with the corresponding refractive indices (for a non-magnetic medium $\eta_i = \sqrt{\varepsilon_i}$), equation (5) becomes:

$$\frac{x_1^2}{\eta_1^2} + \frac{x_2^2}{\eta_2^2} + \frac{x_3^2}{\eta_3^2} = 1 \qquad (6)$$

η_i are called the principal refractive indices and henceforth it will be assumed $\eta_1 \geq \eta_2 \geq \eta_3$: This equation represents the index ellipsoid or optical indicatrix. The three mutually perpendicular semi-axes of this ellipsoid are equal to η_1, η_2, η_3 respectively. It should be noted that η_i is the refractive index for light linearly polarized — not propagated — along the corresponding semi-axis.

With the aid of the index ellipsoid, the orientation of the privileged directions, as well as the phase velocities of the two linearly polarized electro-magnetic waves permitted to propagate unchanged through the anisotropic medium, can be found. They are determined by the intersection of the index ellipsoid with the plane perpendicular to the direction of propagation passing through its centre. This intersection is, in general, an ellipse. The privileged directions coincide with the principle semi-axes η_a, η_b of this ellipse, and the two phase velocities are

$$U_1 = \frac{c}{\eta_a} \quad , \quad U_2 = \frac{c}{\eta_b} \, .$$

The phase difference, per unit length of the anisotropic medium, is

$$\delta = 2\pi\nu\left(\frac{1}{U_1} - \frac{1}{U_2}\right) = \frac{2\pi}{\lambda}\,(\eta_a - \eta_b) \, ,$$

where ν , λ are the frequency and the free space wavelength of the radiation. For any arbitrary direction of propagation, $\eta_a - \eta_b \leq \eta_1 - \eta_3$ and therefore δ takes its maximum value when $\eta_a = \eta_1$, $\eta_b = \eta_3$. This condition, of course, is satisfied only when light is propagated along the η_2 semi-axis of the index ellipsoid.

5. ELECTRO-OPTICAL EFFECT

The value of the six independent components ϵ_{ij} of the dielectric tensor of many crystals, and consequently the shape of their index ellipsoid, can change under the influence of an applied electric field $\overline{E} = [E_1, E_2, E_3]$ through the electro-optical effect. When this is proportional to the applied field, the effect is called the linear electro-optical or Pockels effect. This change is given by:

$$\frac{1}{\epsilon_{ij}} - \left(\frac{1}{\epsilon_{ij}}\right)_{E=0} = r_{ijk} E_k \qquad \left.\begin{matrix} i \\ j \\ k \end{matrix}\right\} = 1,2,3 \, . \qquad (7)$$

The 27 coefficients r_{ijk} are constants of the crystal and constitute the electro-optical tensor. Since $\epsilon_{ij} = \epsilon_{ji}$, it follows that $r_{ijk} = r_{jik}$; therefore the symmetry of the dielectric tensor reduces the number of the components of the electro-optical tensor from 27 to 18. Furthermore, the presence of certain symmetry elements in the crystal restricts some of the r_{ijk} components to zero values. This is the result of a general principle of invariance in crystal physics according to which: 'all expressions involving any physical constant of a crystal should be invariant when any symmetry operation of the crystal is applied'[2].

Using equation (7), equation (4) becomes:

$$\sum \frac{x_i x_j}{\epsilon_{ij}} + \sum r_{ijk} E_k \, x_i x_j = 1 \, . \qquad (8)$$

This is the general form of the equation of the distorted ellipsoid. Equation (8) takes

a simpler form if the original ellipsoid is referred to the system of its principal dielectric axes (after the substitution $\eta_i^2 = \epsilon_i$ has been made):

$$\frac{x_1^2}{\eta_1^2} + \frac{x_2^2}{\eta_2^2} + \frac{x_3^2}{\eta_3^2} + \sum r_{ijk} E_k x_i x_j = 1. \qquad (9)$$

For crystals which belong to the $\bar{4}3m$ point group of the cubic system (with $n_1 = n_2 = n_3 = n_o$) the only non-zero electro-optical coefficients are:

$$\left.\begin{aligned} r_{231} &\equiv r_{321} \\ r_{132} &\equiv r_{312} \\ r_{123} &\equiv r_{213} \end{aligned}\right\} = r_{41} \quad .$$

The equation of the resulting index ellispoid (which in the absence of an electric field is a sphere) is of the form:

$$\frac{x_1^2 + x_2^2 + x_3^2}{\eta_o^2} + 2\, r_{41}\left(E_1 x_2 x_3 + E_2 x_3 x_1 + E_3 x_1 x_2\right) = 1 \; . \qquad (10)$$

Taking the axes (x_1, x_2, x_3) of the original co-ordinate system, parallel with the three crystallographic axes $\langle 100\rangle$, $\langle 010\rangle$, $\langle 001\rangle$ respectively, the orientation of a <u>new</u> coordinate system whose axes are parallel with the directions of the principal refractive indices of the <u>distorted</u> index ellipsoid can be found. Equation (10) in this new system takes the form

$$\frac{x_1^2}{\eta_1^2} + \frac{x_2^2}{\eta_2^2} + \frac{x_3^2}{\eta_3^2} = 1 \qquad (11)$$

The values of η_1, η_2, η_3 are $\eta_i = \sqrt{1/k_i}$ where the k_i are the three roots of the cubic <u>secular equation</u>[3].

$$\begin{vmatrix} \left(\frac{1}{\eta_o^2} - k\right) & r_{41}E_3 & r_{41}E_2 \\ r_{41}E_3 & \left(\frac{1}{\eta_o^2} - k\right) & r_{41}E_1 \\ r_{41}E_2 & r_{41}E_1 & \left(\frac{1}{\eta_o^2} - k\right) \end{vmatrix} = 0 \qquad (12)$$

derived from the matrix associated with the rotational transformation of the coordinate axes.

6. OPTIMUM CRYSTAL ORIENTATION

Using the secular equation, it can be shown that a given electric field induces maximum birefringence, $\Delta\eta = \eta_1 - \eta_3$, when it is applied perpendicularly to <u>any of the (110) (011), (101) planes of the crystal</u>. The components of the electric field $\bar{E}$ in this case are

$$E_1 = E_2 = \frac{E}{\sqrt{2}} \quad , \quad E_3 = 0 \; .$$

Substituting these values in equation (12) it is found that:

$$\begin{aligned} \eta_1 &= k_1^{-\frac{1}{2}} = \left(\frac{1}{\eta_o^2} - r_{41}E\right)^{-\frac{1}{2}} \simeq \eta_o + \tfrac{1}{2} r_{41} \eta_o^3 E \\ \eta_2 &= k_2^{-\frac{1}{2}} = \eta_o \\ \eta_3 &= k_3^{-\frac{1}{2}} = \left(\frac{1}{\eta_o^2} + r_{41}E\right)^{-\frac{1}{2}} \simeq \eta_o - \tfrac{1}{2} r_{41} \eta_o^3 E \; . \end{aligned} \qquad (13)$$

Using the above relations, in a method described by Nye[3], the semi-axes η_1 and η_3 of the index ellipsoid are found to lie on the same plane (110) as the electric field, and to form angles $\pm 45^{\circ}$ with it (see Fig.1). The direction of η_2 along which the light should be propagated is consequently perpendicular to the direction of the electric field. This is the great advantage of the cubic over the uniaxial crystals (i.e. the widely-known KDP crystals where the light has to propagate along the directions of the applied field). Firstly, the design of the electro-optical shutter is greatly simplified (with no need for transparent or specially-shaped electrodes) and, secondly, the required field can be reduced by using crystals whose length L is large compared with the dimensional along which the field is applied. It is apparent, that in any electro-optical shutter employing a cubic crystal of the $\bar{4}3m$ point group (i.e. GaAs, CdTe, ZnSe, etc.) the best performance is achieved when the following conditions are satisfied:

(a) The crystal has its faces parallel with the $(1\bar{1}0)$, (110), (001) crystallographic planes.

(b) The field is applied perpendicularly to the (110) plane.

(c) The laser beam is propagated along the $\langle 1\bar{1}0 \rangle$ axis with its direction of polarization parallel with (or normal to) the direction of the applied field.

The phase difference which is developed between the two components of the linearly polarized light is then given by:

$$\delta = \frac{2\pi L}{\lambda}(\eta_1 - \eta_3) = \frac{2\pi L}{\lambda d} r_{41} \eta_o^3 V \qquad (14)$$

where $V = Ed$ is the amplitude of the applied voltage. When

$$V_{\frac{1}{2}} = \frac{\lambda d}{2L r_{41} \eta_o^3} \qquad (15)$$

$\delta = 180^{\circ}$ and the transmittance of the electro-optical shutter reaches its upper limit $T = T_o$. This value of $V_{\frac{1}{2}}$ is called the half-wave retardation voltage.

Figure 2 shows the Pockels cell used throughout this investigation. The 10 x 10 x 50 mm Gallium Arsenide crystal is mounted in a way that satisfies the above conditions for optimum orientation. Indium foil inserted between the crystal and the two electrodes ensured that the crystal was firmly held without being stressed; otherwise, in the absence of an electric field strain birefringence could be induced.

Using equation (15) and the values of $\lambda = 10.6\,\mu m$, $r_{41} = 1.4 \times 10^{-10}$ cm V^{-1} $\eta_o = 3.3$. the half-wave retardation voltage of this Pockels cell is determined as:

$$V_{\frac{1}{2}} = 21.06\,kV .$$

7. EXTINCTION RATIO

Although in theory there should be no transmission of light through an electro-optical shutter in the absence of an electrical field, in practice there is always a small transmittance arising from optical imperfections in the system of polarizers and the electro-optical crystal (residual strain-induced birefringence).

The ratio of the intensity I_o of the radiation incident on the second polarizer (see Fig.3) to the transmitted intensity I when no field is applied, is called the extinction ratio of the electro-optical shutter ($E_s = I_o/I$). The value of E_s is an

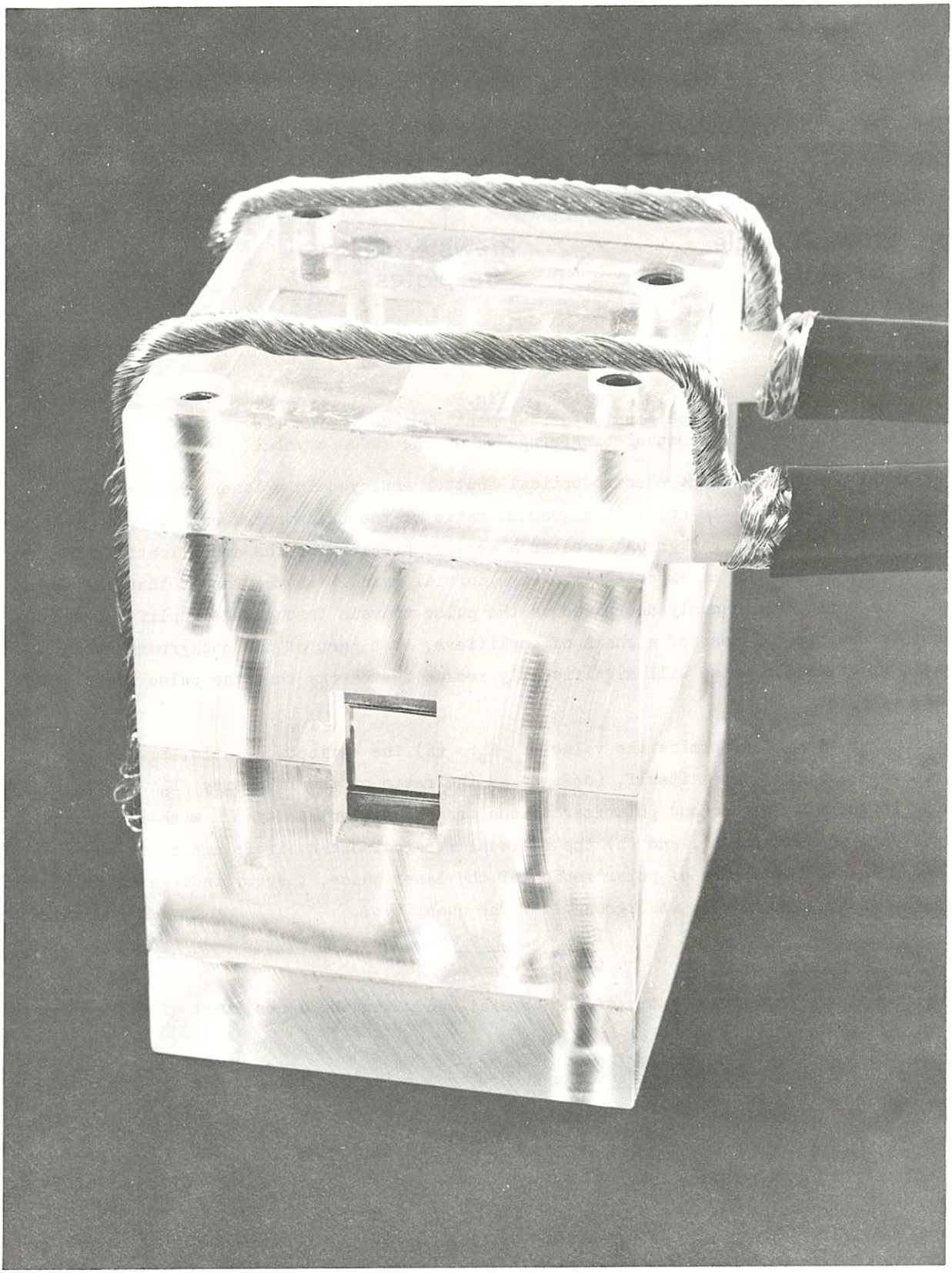

Fig.2
GaAs Pockels Cell

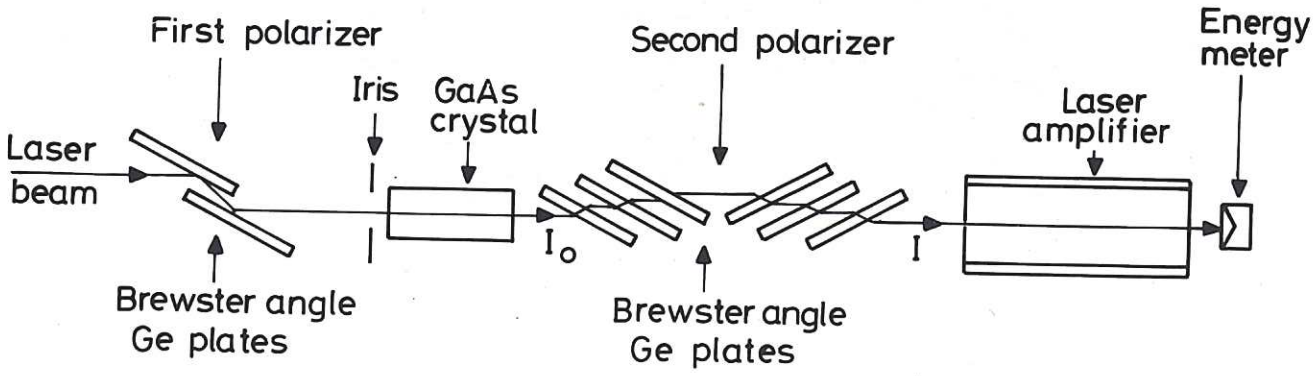

Fig.3
Experimental arrangement for measuring the residual birefringence of the GaAs crystal

important parameter of the electro-optical shutter employed in a laser system since it determines the signal-to-noise (background) ratio of the transmitted pulse. The presence of this low intensity background creates a serious problem for the amplification of nanosecond pulses because it experiences a high initial gain, with the result that the signal-to-noise ratio continuously decreases as the pulse travels through the amplifying medium. Furthermore, in the case of a chain of amplifiers, that part of the background which is ahead of the short pulse will significantly reduce the energy that the pulse would otherwise extract.

Two factors determine the value of E_s: (a) the extinction ratio, E_p, of the crossed polarizer system itself, (defined as the ratio of the intensity I_o' of the radiation incident on the second polarizer to the transmitted intensity I' with the crystal removed from the system), and (b) the residual strain-induced birefringence in the crystal which reduces the degree of polarization of the laser pulse, thereby increasing the leakage of the unwanted radiation (background). The quantity:

$$E_c = \left(\frac{1}{E_s} - \frac{1}{E_p}\right)^{-1} \tag{16}$$

represents the extinction ratio of the crystal and gives the upper limit of the extinction ratio of the system as a whole.

Using the Fresnel formulae, the theoretical value of E_p, for the system of polarizers shown in Fig.3, was derived as:

$$E_p = \left(\frac{\eta^4 + 1}{2\eta^2}\right)^m \tag{17}$$

where m is the number of plates which comprise the second polarizer. An experimental arrangement for measuring the values of E_p and E_s is also shown in Fig.3.

When the second polarizer and the GaAs crystal were removed, the intensity I_o' was measured. After the polarizer had been replaced, the very low intensity I' of the transmitted radiation was amplified by activating the laser amplifier and, subsequently, reached a measurable level. Taking into account the known gain of the amplifier, the extinction ratio in the case of three, four and five Ge plates, comprising the second polarizer, was

found to be:

$$E_{p3} = 560 \ , \quad E_{p4} = 4{,}600 \quad \text{and} \quad E_{p5} \geq 10^4 \ .$$

These values closely agreed with the theoretical values deduced from equation (11). This fact indicates the very high degree of polarization of the radiation reflected from the first polarizer, and also allows a value of $E_{p6} > 10^5$ to be estimated when six plates are used.

Replacing the crystal, the extinction ratio E_s of the electro-optical shutter as a whole was similarly measured and, using equation (16) the value of E_c was deduced.

Three GaAs crystals, with dimensions 10x 10x 50 mm were tested and the values of their E_c, with the full cross-section of the crystals exposed to the radiation, were found to be 400, 600, and 3,400 respectively. When the exposed area of the crystal was reduced by placing an iris symmetrically in front of it, the values of E_c were found to be considerably higher. This clearly shows that the quality of the crystal is poorer near the edges and according to Figueira[4] this is due to strains introduced during the cutting and polishing processes. In the same study, a similarly large sample-to-sample variation in the quality of the GaAs crystals, was also found.

8. LASER TRIGGERED SPARK GAP

The advantages of the laser-triggered spark-gap over the conventional electrically-triggered switch were widely recognised soon after the first experiments in initiating a spark discharge by focussing a laser beam into a d.c. charged spark gap, were reported[5]. These advantages can be itemised as:

(a) the absence of electrical coupling between the triggering device (i.e. the laser) and the high voltage assembly;

(b) the very short delay time (of the order of a few nanoseconds) and its subnanosecond variation (jitter) from shot-to-shot;

(c) the capability of simultaneously triggering several LTSG's; and

(d) the very simple, robust and compact structure — as well as the long life — of the LTSG.

Although the use of an LTSG as a general purpose high-speed switch would be somewhat extravagant, considering the high cost of lasers, it is nevertheless ideal for applications such as the generation of short laser pulses. In such an application, the laser pulse itself provides the triggering of the spark gap via a beam-splitter, thus achieving the necessary high degree of synchronisation without the need for a separate triggering device.

Gas-filled spark gaps appear to be preferable to liquid or solid dielectric-filled gaps and have been much more thoroughly investigated[13,20].

The main disadvantage of the liquid dielectric-filled spark gap is that it has a delay time of several microseconds, compared with the nanosecond response of the gas-filled pressurized gap.

Gaps insulated with solid dielectric have the drawback that the dielectric must be replaced after each gap closure since it lacks self-healing properties.

For the gas-filled spark gap, a pressurized gap is preferable to a low or atmospheric pressure spark gap for two reasons:

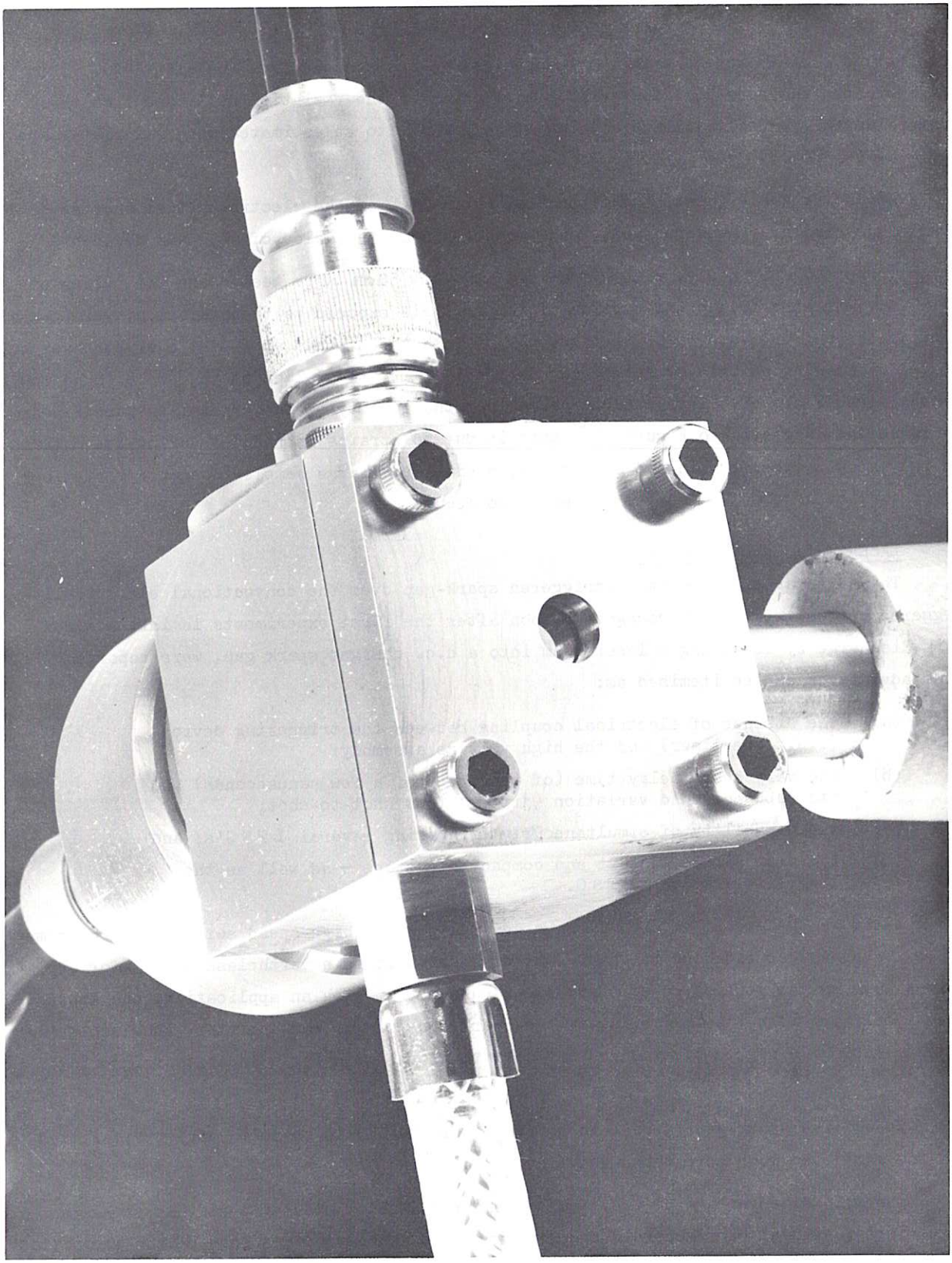

Fig.4

High-pressure L T S G

(a) the time taken for the development of the conduction path is reduced by increasing the pressure for a given value of V/V_{sb} (where V is the charging voltage and V_{sb} the self breakdown voltage of the gap);

(b) by increasing the gap pressure, the gap spacing required to hold off a certain voltage decreases (Paschen's Law) resulting in a faster rise-time of the electrical pulse generated by the gap closure (as will be shown later).

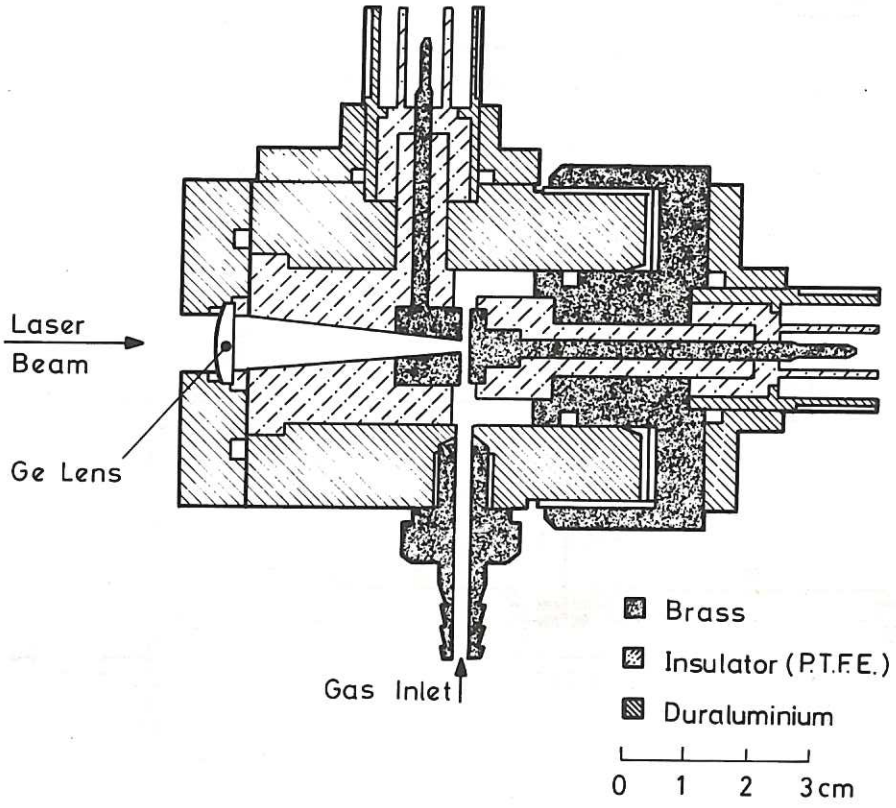

Fig.5
Cross-section of the LTSG

The coaxial structure of the LTSG used (see Fig.4) is shown in cross-section in Fig.5. The laser beam is directed on the cathode disc via a 2 mm central hole in the anode, using a plano-convex Ge lens as combined window and focusing element. The lens was so chosen that its focal point would lie ~2 mm behind the target electrode. This arrangement, according to Bettis et al[6], results in the minimum delay time and jitter. The gap spacing is adjustable by means of a 6.67 turns per centimetre thread on the main body of the LTSG, and is effected by rotating the main ring bearing the cathode assembly.

Nitrogen at pressures up to 7000 torr was used as the insulating gas. An uncoated Ge flat was placed at 45° in front of the LTSG and the reflected beam was monitored using a calibrated photon-drag detector (Rofin model 7415). The intensity of the laser beam transmitted through the lens was easily estimated from the detector readings by using the Fresnel formulae to calculate the reflection loss which the beam suffers from both the Ge flat and the uncoated lens.

A single longitudinal, single-transverse, mode TEA CO_2 laser[7] was used to trigger the spark-gap. The normal duration of the pulse was 70 ns, although this could be adjusted within the range 60-200 ns by changing the gas mixture. The peak power of the

transmitted beam could be attenuated from 2 MW to zero. The smooth time profile of this laser pulse is essential for the accurate measurement of LTSG parameters such as delay time, jitter and threshold power for breakdown. The spontaneous mode-locking that normally occurs in a T E A CO_2 laser, and the difficulty of its removal, might account for the paucity of data on delay time and jitter measurements in the literature, in contrast with the numerous measurements pertaining to ruby, dye, YAG and Nd glass lasers.

9. PULSE GENERATOR

A pressurised spark-gap similar to that reported by Alcock et al[8] was employed as the switch in a transmission-line pulse generator (Fig.6) of a type first described in 1949 by R.C. Fletcher[9], who used it as here to produce multi-kilovolt pulses with a sub-nanosecond risetime.

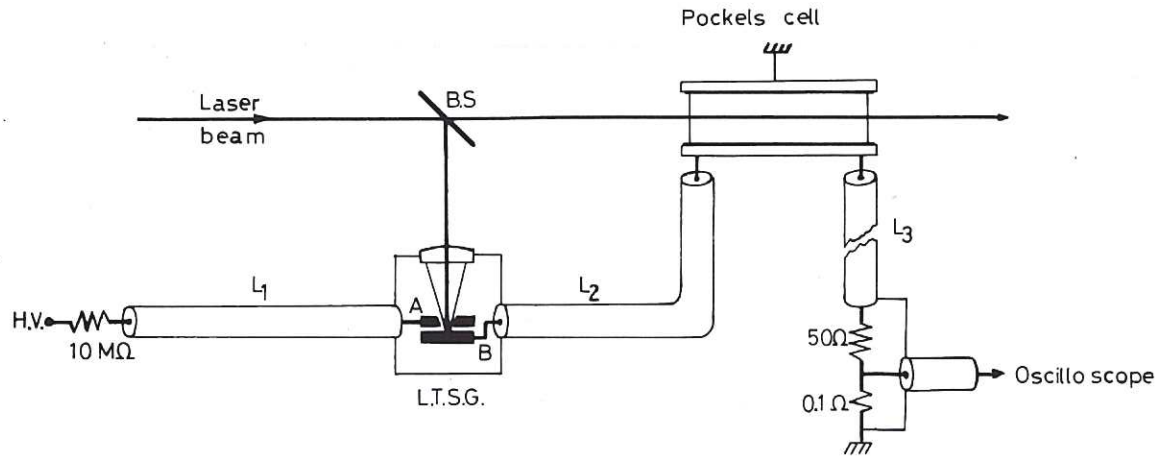

Fig.6
Multi-kilovolt transmission-line type nanosecond pulse generator

The distributed capacitance of the high frequency coaxial cable L_1 is charged from a high voltage d.c. power supply through a resistor $R_1 = 10^7\ \Omega$. The other end of the cable is connected, at point A, to one of the electrodes of a pressurised LTSG. The electrode spacing and gap pressure are such that the self-breakdown voltage V_{sb} of the gap is higher than the potential $V_A = V_o$ to which the cable is charged. The potential on the second electrode of the gap is $V_B = 0$. When the gap is triggered by the laser beam at the time $t_1 = 0$ the potentials at the points A and B are equalised: $V'_A = V'_B$.

Since the potential V_B at the point B was originally zero, the gap closure is equivalent to a short circuit appearing at one end of a charged line[10] and therefore $V'_A = V_A/2 = V_o/2$. As a result, two similar ramp functions of opposite sign are generated at the switching point. These propagate out in opposite directions along the lines L_1 and L_2 with amplitudes

$$V_1 = \frac{V_o}{2} - V_o = -\frac{V_o}{2} \quad \text{and} \quad V_2 = \frac{V_o}{2} - V_o = \frac{V_o}{2} \ .$$

Both waves travel with the group velocity U of the line which is:

$$U = c/\sqrt{\varepsilon}$$

where c is the velocity of electromagnetic waves in free space, and ε is the relative

dielectric constant of the insulating medium between the two conductors of the line. The dielectric in the cables used here was polyethylene, for which $\varepsilon = 2.3$ and therefore $U = 0.66\,c \simeq 1.98 \times 10^8$ m/s.

The positive amplitude of the wave on the line L_2 imposes a step voltage $V_o/2$ as it travels through it, whereas the negative wave discharges the voltage on the line L_2 to half of its original value as it travels towards the charging resistor R_1 where it arrives at time $t_2 = L_1/U$. Because of the impedance mis-match, it is reflected at this point, and travels back along L_1. The reflection coefficient is given by

$$\rho = \frac{R_1 - Z_o}{R_1 + Z_o} \qquad (18)$$

where $Z_o = 50\,\Omega$ is the characteristic impedance of the transmission line. With $R_1 = 10^7\,\Omega \gg Z_o$, the reflection coefficient $\rho = 1$ and the reflected wave remains negative with the same amplitude $(-V_o/2)$. Thus the reflected wave completes the discharge of the line L_1 as it returns to the LTSG, where it arrives at the time $t_3 = 2L_1/U$ and cancels the positive potential $V_o/2$ at B.

Since the positive wave has already been travelling for a similar time $2L_1/U$ before being cancelled by the negative wave, the net result is clearly the generation of a rectangular pulse of height $V_o/2$ and width $t = 2L_1/U$ on the line L_2, leading to the Pockels cell. A rigorous mathematical treatment of this type of pulse generator can be found in reference (11).

This electrical pulse, having propagated along the line L_2, over the electro-optical crystal and through L_3, arrives at the terminating resistor R_2. With the values of R_2 and R_3 chosen such that $R_2 + R_3 = Z_o$, the pulse will be absorbed because reflectivity $\rho = 0$ for an impedance match (equation (18)). Thus there can be reflection of the pulse to activate the electro-optical crystal further.

The two resistors R_2 and R_3 ($R_3 \ll R_2$) form a voltage divider to attenuate the multi-kilovolt pulse to an amplitude suitable for oscilloscope display. By varying the length of the line L_1 from 0.15 to 10 metres, electrical pulses of duration ~ 1.5 to 100 nanoseconds are readily achieved. A Tektronix 519 Oscilloscope with a deflection sensitivity of 9.8 V/div and a rise time of 0.29 ns was used to display these pulses (Fig.7). Because the duration of the voltage pulse depends solely on the length and the dielectric material of the transmission line L_1, this pulse generator has a remarkable stability usually lacking in generators using active elements.

10. MECHANISM OF THE LASER-INDUCED GAP BREAKDOWN

The breakdown mechanism proposed by Guenther et al[12] seems more likely to apply to the present case than those suggested by other investigators[13,14] and will be described first. In this mechanism, it is assumed that the electrons generated by focusing the laser on to the target electrode (section 7), drift across the gap under the influence of the applied electric field and, in so doing, gain sufficient energy to ionize the gas molecules or atoms by collision. The growth of ionization conforms to the Townsend classical avalanche process according to which the number of electrons N produced after a distance x is:

$$N = N_o \exp(\alpha x)\,. \qquad (19)$$

Here, N_o is the number of electrons emitted from the electrode and α is the first Townsend

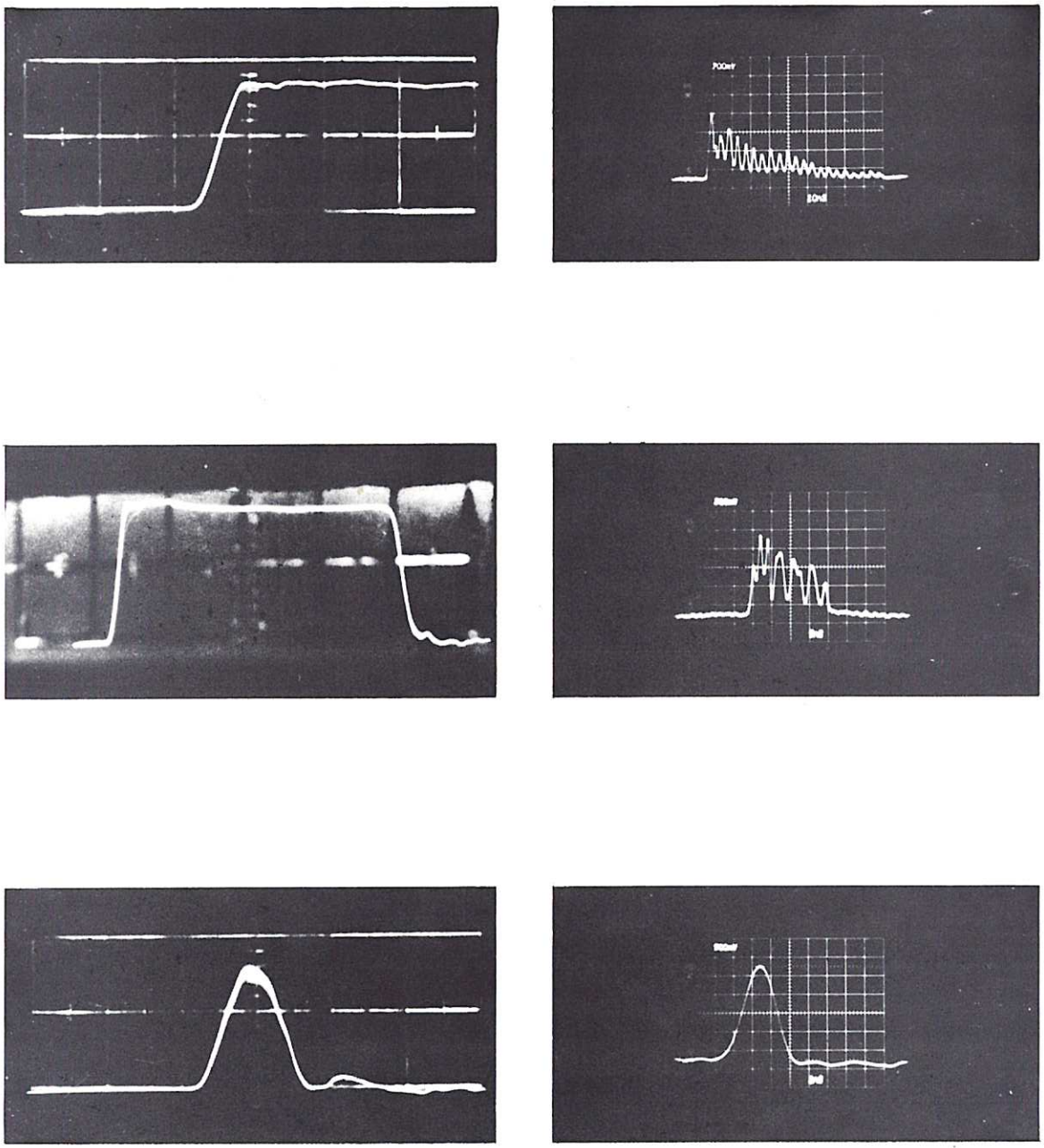

Fig.7

Typical examples of the generated CO_2 laser pulses — on the right — (10 ns/div ; 5 ns/div; 1 ns/div, from top to bottom) together with the corresponding electrical pulses which activate the Pockels cell — on the left — (2 ns/div; 5 ns/div; 2 ns/div , from top to bottom)

ionization coefficient (i.e. the number of ionizing collisions per centimetre made by one electron travelling in the electric field direction). This process continues until the entire gap is bridged with an ionized conducting path. The velocity of the avalanche v_a is considered as equal to the electron drift velocity ($v_a \sim 10^7$ cm/sec). This mechanism, however, fails when the measured delay time is shorter than the time required for the avalanche to travel a distance equal to the gap length d. In such a situation the more rapid 'streamer' mechanism is required to account for the temporal behaviour of the breakdown. In this process according to Raether[15], the electron multiplication follows the avalanche process until the number of electrons reaches a critical value $N_c \simeq 10^8$ after a distance of travel x_c. At this stage the avalanche is transformed into a plasma streamer advancing rapidly with a velocity $v_s \sim 10^8$ to 10^9 cm/sec. The total formative time, which can be defined as the period of time that elapses between the creation of the electrons on the target electrode and the appearance of the high voltage on the opposite electrode, may therefore be expressed as:

$$t_f = \frac{x_c}{v_a} + \frac{d - x_c}{v_s}$$

or using equation (19)

$$t_f = \frac{\ell n(N_c/N_o)}{v_a} + \frac{d - x_c}{v_s} \qquad (20)$$

11. DELAY TIME AND JITTER

The delay time, t_d, of a LTSG — defined as the period of time between the arrival of the laser pulse on the target electrode and the appearance of the electrical pulse on the opposite electrode — may be considered as the sum of two smaller periods of time:

(a) the time, t_e, needed for the laser to heat the target material to its melting point T_m (i.e. the time needed for the emission of the N_o electrons); and

(b) the formative time, t_f, which has already been defined.

In the present case where the CO_2 laser pulse has a slow rise time (~70 ns) the value of t_e can be readily shown to be comparable with — or even greater than — the value of t_f and cannot therefore be overlooked as it can with laser pulses of a few picoseconds[16] or a few nanoseconds[10] duration.

As will be seen later,

$$t_e = \frac{K}{P^2}$$

where

$$K = \frac{T_m^2 \pi \rho c k}{4A^2}$$

is a thermal constant of the target material, and P is the incident laser power density Thus, using equation (20), the delay time $t_d = t_e + t_f$ is:

$$t_d = \frac{T_m^2 \pi \rho c k}{4A^2} \frac{1}{P^2} + \frac{\ell n N_c - \ell n N_o}{\alpha v_a} + \frac{d - x_c}{v_s} \qquad (21)$$

The above equation predicts the effect which variations in laser intensity, applied voltage, gap spacing and pressure will have on the delay time. A reasonable agreement between the predicted and the experimental response was observed.

As a result of an increase in laser power, shorter values of t_d were recorded, presumably because of the smaller value of t_e. Fig.8 indicates the effect of the charging

voltage of the gap, V, on the delay time. The observed increase in the delay time with decreasing V is clearly due to the fact that both α and v_a decrease with the decreasing field.

When the pressure p was increased simultaneously with a decrease in the gap spacing, keeping the ratio E/p constant, a decrease in the value of t_d was observed. This result also is anticipated by equation (21) since the Townsend coefficient α is proportional to the pressure p for constant E/p.

It is thus apparent that in order to minimise the delay time of a CO_2 LTSG, the highest permissible values of laser power and pressure should be used in conjunction with a charging voltage as near to the self-breakdown value as possible.

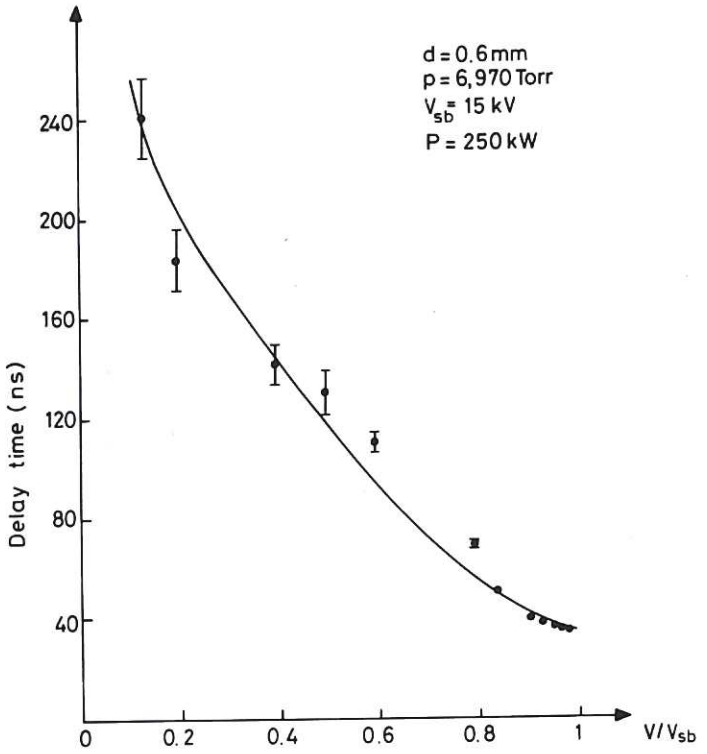

Fig.8
Delay time as a function of the applied voltage

The error bars in Fig.8 indicate the maximum jitter of the delay time. Subnanosecond jitter is observed for $V \geq 0.8\ V_{sb}$. It should be noted here however, that the jitter remains low only if the power of the incident laser pulse does not change from shot-to-shot. Any variation of the laser power results in a considerable increase of the jitter even when $V \geq 0.8\ V_{sb}$. This is apparently caused by changes in the value of t_e, which is dependent on laser power. The peak power of the laser beam which entered the gap when the measurements in Fig.8 were taken was 250 kW. The minimum power required to trigger the gap when the charging voltage $V \simeq 0.95\ V_{sb}$ was found to be $\sim$ 20 kW, corresponding to a threshold energy of 1.5 mJ.

12. ELECTRODE MATERIAL

Since the electron emission from the target electrode is regarded as thermionic[17,18,19,25], the constants of the material which affect the rate of laser heating — and therefore the electron emission — must be considered when choosing the most suitable material for achieving the shortest possible delay time, t_d. When the target electrode is irradiated by a 'triangular' laser pulse of duration τ, the temperature T at the surface, as a function of time $t(t \leq \tau)$ is given by the relation[20]:

$$T = \frac{2AP}{\sqrt{\pi \rho ck}}\, t^{\frac{1}{2}} \qquad (22)$$

where A is the absorbed fraction of the incident radiation, P the laser power density and ρ,c,k the density, specific heat and thermal conductivity of the electrode material respectively.

Tungsten has been claimed as the best material for spark gaps triggered by laser radiation of up to 1 μm wavelength[19,20] with aluminium, brass and stainless steel in descending order of desirability. However, the longer wavelength of the CO_2 laser (10 μm) requires the resistivity of the material to be taken into account, for this determines the value of the absorption A [21]: i.e.

$$A = 3.65 \times 10^{-3} (R/\lambda)^{\frac{1}{2}} \qquad (23)$$

where λ is the wavelength in μm and R is the resistivity in Ω.μm. Using the relations (22) and (23) to ascertain the comparative rates of laser heating, the different electrode materials can be listed in order of desirability for $\lambda \sim 10$ μm as: stainless steel, tungsten, brass, aluminium and copper.

Although brass electrodes were used in the present case, they were found to be quite satisfactory for the generation of nanosecond pulses because for any value of the charging voltage $V \geq 0.7\ V_{sb}$ the electrical pulse appears on the output of the LTSG before the laser pulse reaches its peak (see Fig.8). By suitably delaying the electrical pulse, its arrival on the Pockels cell can be arranged to coincide with the peak of the laser pulse.

13. RISE TIME DEPENDENCE ON GAS TYPE, PRESSURE, GAP SPACING AND CHARGING VOLTAGE

While there has been thorough investigation of the delay time and jitter in LTSG operation — notably the articles by Guenther et al[12,20] proposing how they can be optimized — there is very limited experimental evidence[22] of the effect of spark gap parameters — such as gas pressure and operating voltage — upon the rise time of the electrical pulse.

Bearing in mind the fact that the rise time of the transmitted laser pulse will be determined by that of the electrical pulse, it is clearly important that the operating conditions for the minimum rise time should be found.

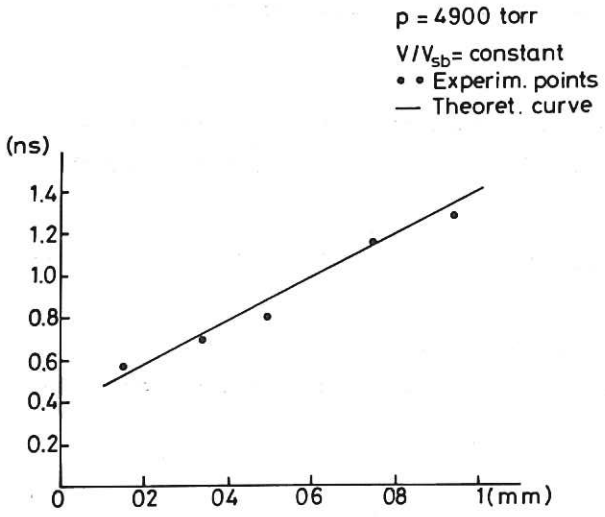

Fig.9
Effect of the gap spacing on the rise time of the electrical pulse

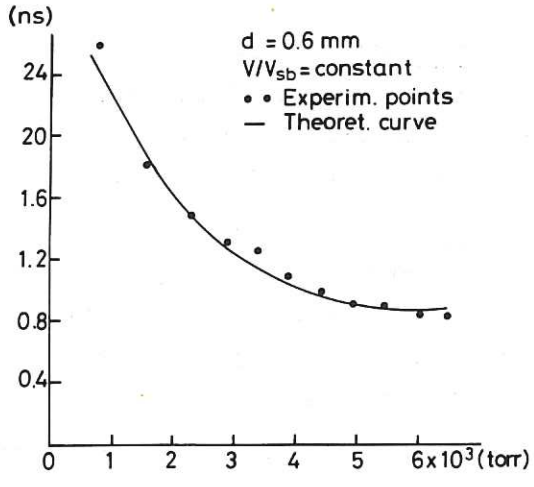

Fig.10
Effect of the nitrogen pressure on the rise time of the electrical pulse

Figures 9 and 10 illustrate the effect of the gap spacing and the gas pressure respectively on the rise time of the electrical pulse. The gas pressure was held constant for the former and the gap spacing for the latter. The ratio V/V_{sb} was maintained at a constant value in both cases.

The solid lines are theoretical curves based on the relation[22]

$$t_R = 3.5\, p d^2/SV^2 \qquad (24)$$

which gives the rise time as a function of the gap spacing d, the gas pressure p and the applied voltage V. The best fit to the experimental points gives a value for the constant S of 440 torr cm^2 V^{-2} s^{-1}. The close agreement (a) between this value of S and those of 418 ± 10% torr cm^2 V^{-2} s^{-1} [23] and 450 torr cm^2 V^{-2} s^{-1} [22] in other investigations, and (b) between the measured and the predicted values of the rise time, fully endorses the validity of equation (24).

Nitrogen was chosen as the insulating gas because of its high dielectric strength. It has often been suggested[10,20,23] that a mixture of nitrogen and argon (which has a lower dielectric strength should be used in order to achieve shorter delay times. However the addition of argon was avoided, in the present case, for two reasons:

(a) because there is no need for any further reduction in the delay time while the maintenance of as short a rise time as possible is essential;

(b) because this will necessitate longer gap spacings to hold off the same voltage, which, in turn, will increase the rise time of the electrical pulse. It can be easily shown that the rise time will be increased by a factor of 1 to 5.3 should the argon concentration change from zero to 100%.

Should the need arise in future applications of the CO_2 LTSG for even shorter delay time, this could be achieved — without any adverse effect on the rise time of the electrical pulse — by replacing the brass electrodes with those of stainless steel, rather than by adding argon to the nitrogen.

Equation (24) indicates how any change in the voltage applied across the gap affects the rise time of the electrical pulse (i.e. for constant pressure and gap spacing: $t_R \propto \frac{1}{V^2}$). Thus operation as near self-breakdown as possible is essential not only to obtain shorter delay time but, more importantly, to achieve faster-rising electrical pulses.

14. CONCLUDING REMARKS

The electro-optical shutter, whose operational characteristics are fully analysed here, has been used to generate single subnanosecond CO_2 laser pulses from the output of a self-mode locked oscillator[26].

Figure 7 shows three laser pulses (on the right) of duration 100, 20 and ~1.5 nsec transmitted by the shutter, together with the corresponding electrical pulses (on the left) that activated the GaAs crystal. The performance of the device has shown no signs of deterioration after two years of use. However there are some improvements which could be made in the existing arrangement:

1. The main limitation in its performance is the finite contrast ratio (signal/background noise) of the switched-out laser pulses due to the intrinsic birefringence of the GaAs crystal. The upper limit of this ratio (i.e. the extinction ratio of the crystal) is attained when the voltage of the electrical

pulse is made equal to the half-wave retardation voltage $V_{\frac{1}{2}}$ (in the present case $V_{\frac{1}{2}} = 21$ kV). Up to now the voltage used has been $V \simeq \frac{1}{3} V_{\frac{1}{2}}$, and therefore increasing this will significantly improve the present contrast ratio. However, this should be followed by an appropriate increase in the pressure of the nitrogen in the spark gap in order to maintain the fast rise time of the electrical pulse (see equation (24)).

2. As a further step to improve the contrast ratio, a second GaAs crystal could be used together with an additional polarizer. This should greatly improve the contrast ratio because the upper limit in this case will be determined by the product of the extinction ratio of the two crystals: $E_c = E_c^{(1)} \times E_c^{(2)} \sim 10^8$.

ACKNOWLEDGEMENTS

The authors particularly wish to record their appreciation of Dr V.I. Little's gentle encouragement throughout the course of this work, and his valuable guidance in the recording of it. One of us (T S) is grateful for the support of a studentship at Culham, where the shutter was developed.

REFERENCES

(1) BORN, M. and WOLF, E., 'Principles of Optics', Pergamon Press, 4th ed. (1970).

(2) RAMACHANDRAN, G. N. and RAMESESHAN, S., 'Crystal Optics', In Handbuch der Physik, vol. 25/1, Berlin: Springer-Verlag, p.192 (1961).

(3) NYE, J. F., 'Physical Properties of Crystals', Oxford:Clarendon Press, pp.41-42 (1957).

(4) FIGUEIRA, J. F., IEEE J. Quantum. Electron., QE-10, 572 (1974).

(5) PENDLETON, W. K. and GUENTHER, A. H., Rev. Sci. Instr., 36, 1546 (1965).

(6) BETTIS, J. R. and GUENTHER, A. H., IEEE J. Quant. Electron., QE-6, 483 (1970).

(7) STAMATAKIS, T. and SELDEN, A. C., Phys. Letts., 58A, 221 (1976).

(8) ALCOCK, A. J., RICHARDSON, M. C. and LEOPOLD, K., Rev. Scient. Inst., 41, 1028(1970).

(9) FLETCHER, R. C., Rev. Scient. Instr. 20, 861 (1949).

(10) BEWLEY, L. V., 'Travelling Waves on Transmission Lines', John Wiley & Sons Inc., New York, p.318 (1951).

(11) POTTER, J. L., and FICH, S. J., 'Theory of Networks and Lines', Prentice-Hall Inc., New Jersey, p.398 (1963).

(12) GUENTHER, A. H. and BETTIS, J. R., IEEE J. Quant. Electron., QE-3, 584 (1967)

(13) NOGUCHI, T., YANO, M., SHIMOMURA, T. and HORII, K., Electr. Engin. in Japan 92-A 27 (1972).

(14) PINNEKAMP, F., HIMMEL, G. and BERGSTEDT, K., Opt. Commun., 11, 225 (1974).

(15) RAETHER, H., 'Electron Avalanche and Breakdown in Gases', Washington D.C., Butterworth, (1964).

(16) DEWHURST, R. J., PERT, G. J. and RAMSDEN, S. A., J. Phys. D: Appl. Phys., 5, 97 (1972).

(17) STEINMETZ, L. L., Rev. Scient. Instr., 39, 904 (1965).

(18) NURMIKKO, A. V., IEEE J. Quant. Electron., QE-7, 470 (1971).

(19) KHAN, S. H. and WALSH, D., J. Phys. D: Appl. Phys., 4, 344 (1971).

(20) GUENTHER, A. H. and BETTIS, J. R., Proc. IEEE, 59, 689 (1971).

(21) KIMMITT, M. F., 'Far Infrared Techniques', Pion Ltd., p. 12 (1970).

(22) IRELAND, C. L. M., J. Phys. E: Scient. Instr., 8, 1007 (1975).

(23) HESS, H. and DEPARADE, W., Proc. 3rd Int. Conf. on Gas Discharges, London, IEE Conference Publication No. 118, 136 (1974).

(24) DEUTSCH, F., J. Phys. D: Appl. Phys., 1, 1711-9 (1968).

(25) COBB, J. K. and MURAY, J. J., Brit. J. Appl. Phys., 16, 271 (1965).

(26) LITTLE, V. I., SELDEN, A. C. and STAMATAKIS, T., J. Appl. Phys., 47, 1295 (1976).

HER MAJESTY'S STATIONERY OFFICE

Government Bookshops

49 High Holborn, London WC1V 6HB
13a Castle Street, Edinburgh EH2 3AR
41 The Hayes, Cardiff CF1 1JW
Brazennose Street, Manchester M60 8AS
Wine Street, Bristol BS1 2BQ
258 Broad Street, Birmingham B1 2HE
80 Chichester Street, Belfast BT1 4JY

Government publications are also available through booksellers